Electronic Supplementary Information for "The Verwey structure of a natural magnetite"

G. Perversi, J. Cumby, E. Pachoud, J. P. Wright and J. P. Attfield

Experimental Details

Microcrystal diffraction data were collected on instrument ID11 at ESRF. The experimental procedure was the same as used by Senn et al.5 Microcrystals with radii in the range 10-50 µm were initially screened for diffraction quality at room temperature, and an approximately cuboidal 60 x 50 x 25 µm grain was selected for low temperature study using a nitrogen cryostream. The presence of a long range structural Verwey transition was confirmed by the appearance of sharp superstructure peaks in detector images on cooling, as shown in Fig. S1. Diffraction images from the selected microcrystal were acquired at 90 K with varying angular step, exposition times, beam intensity, and phi settings, to observe a large region of reciprocal space including intense low angle fundamental peaks and weak high angle superstructure spots, and to ensure a good level of redundancy in the dataset. A magnetic field was applied while cooling from 130 to 90 K to minimise twinning of monoclinic domains. The detector images showed that the low-temperature microcrystal had a unique c-axis, and proportions of a/-a, a/b and a/-b type twin domains were determined as part of the structure refinement.

The full 90 K data set consists of 45904 symmetry unique reflections out to a resolution of 0.30 Å. Data reduction was performed using SMART/SAINT software, empirical absorption correction applied in SADABS and incidence angle corrections were performed. Structure refinements were performed in SHELXL 1 taking the Senn et al. 5 model as the initial starting coordinates. All atomic coordinates were refined freely in space group Cc. Refinements were performed with anisotropic thermal parameters for all atoms. The total number of refined parameters including twin fractions was 507. The refined parent domain fraction was 91.9% with 2.9% of a/-a, 2.8% of a/b twin and 2.3% of a/-b twin domains also present. The overall quality of the microcrystal of natural magnetite is very good and comparable to the synthetic pure magnetite studied previously, with a small amount of twinning that can be accounted in the pseudo- merohedral approximation. Structural results are shown in Tables S1 to S4 and orthorhombic distortion mode values are plotted in Fig. S2

Electron Probe Microanalysis (EPMA) was performed using a Cameca SX100 instrument. The cation composition of the bulk sample was obtained by averaging analyses from approximately 100

microcrystal fragments. The average composition and statistical standard deviations are shown in Table 1. Magnetic susceptibility of the powdered bulk magnetite is shown in Fig. S3.

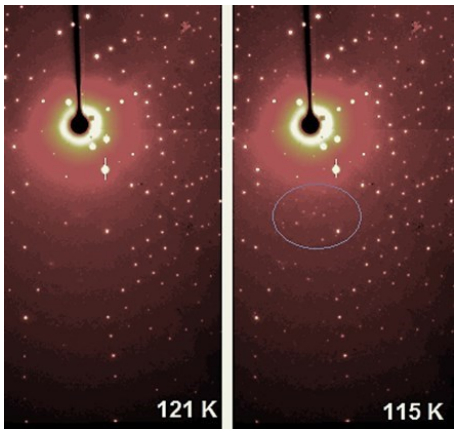

Fig. S1 - Changes in X-ray diffraction data from the natural magnetite crystal around the Verwey transition at T_V = 119 K. Consecutive detector images recorded while cooling through the transition at a rate of 0.5 $Kmin^{-1}$ show the appearance of superstructure reflections such as in the circled region.

Fig. S2 - Distortion amplitudes of the orthorhombic mode, plotted against the radial mode for the 16 octahedral B sites in the Cc structure of the present mineral sample and the pure magnetite of Senn et al.[5] Points for the same B-site in the two structures are connected by lines. Domains of the 8 Fe^{2+}-like and 8 Fe^{3+}-like sites are shown as rectangles. An approximate BVS scale is shown at the top of the plots. The orthorhombic amplitude Q_o is not coupled to the orbital or charge order and reflects secondary distortions due to the high connectivity of the network of FeO_6 octahedra. Hence the values for the two structures are very similar.

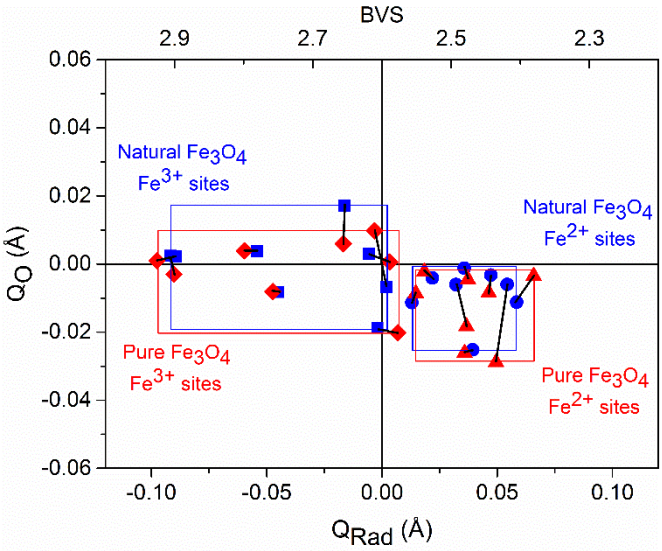

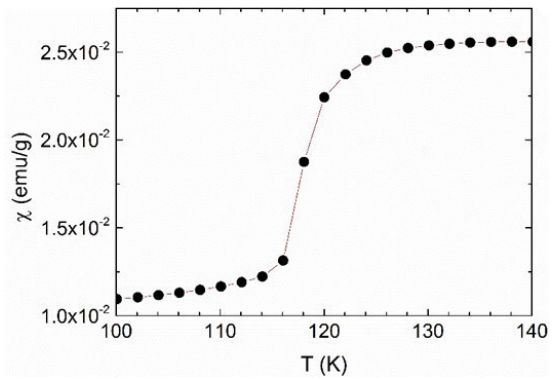

Fig. S3 - Magnetic susceptibility of the powdered bulk magnetite in an applied field of 100 Oe. The transition is broader than for the microcrystal fragment in Fig. 2b, showing that the microcrystal is more homogenous than the powdered sample.

Table S1 - Summary of experimental and refinement details for structure analysis of the natural magnetite grain in the monoclinic Cc phase at 90 K, below the Verwey transition.

Crystal Data	
Chemical Formula	Fe_3O_4
Cell setting, Space group	Cc
Temperature (K)	90.00(2)
a,b,c (Å)	11.8801(17), 11.8457(17), 16.7773(30)
β (°)	90.267(9)
Volume (Å^3)	2361.01(7)
D_c(g cm^{-3})	5.238
X-ray wavelength (Å)	0.15842(1)
μ (mm^{-1})	0.19
Crystal form	Approximately spherical
Crystal size (mm)	r = 0.062, 0.05, 0.025
Data Collection	
Diffractometer	ID11@ESRF, Huber Omega and phi axis
Data collection method	ω
Absorption correction	none
T_{min}	0
T_{max}	0
No. of observed, symmetry unique reflections	180686, 45904
θ_{max} (°)	15.36
R_{int}	0.0422
Range of h,k,l	-39 → h → 39
	-39 → k → 39
	-55 → l → 55
Refinement	
Refine on	F^2
R(F^2), R[F^2 > 4 sigma], wR(F^2), S	0.0416, 0.0359, 0.0890, 1.014
Cutoff: I >σ	none
No. of reflections	93108
No. of parameters	507
Weighting scheme	Weight = 1 / [sigma^2(F_o^2) + (0.0194 * P)^2 + 1.10 * P] where P = (Max (F_o^2, 0) + 2 * F_c^2) / 3
(Δ/α)mean	0.001
(Δ/α)max	0.007
Δρmax, Δρmin (e Å^{-3})	5.88, -5.03
Twin law	(0 -1 0) (1 0 0) (0 0 -1) Applied three times to account for *a/b, a/-a* and *a/-b*
Twin fractions:	0.0280(4) *a/b*, 0.0294(6) *a/-a,* 0.0235(4) *a/-b*

Table S2 - Fractional coordinates and equivalent isotropic thermal parameters.

Sites	x	y	z	U_{eq} (Å^2)
A11	0.87525(2)	0.75138(2)	0.06523(2)	0.00229(2)
A12	0.87803(2)	0.25212(2)	0.06490(2)	0.00216(1)
A13	0.62485(2)	0.75223(2)	0.43791(2)	0.00241(2)
A14	0.62669(2)	0.25361(2)	0.43780(2)	0.00232(2)
A21	0.87470(2)	0.50440(2)	0.19017(2)	0.00218(2)
A22	0.88065(2)	0.00072(2)	0.18839(2)	0.00215(2)
A23	0.62540(2)	0.50148(2)	0.31125(2)	0.00248(2)
A24	0.62907(2)	0.00475(2)	0.31273(2)	0.00243(2)
B1A1	0.75081(2)	-0.00164(3)	0.00153(2)	0.00281(1)
B1A2	0.75133(2)	0.49905(3)	0.0005(2)	0.00266(1)
B1B1	0.00221(2)	0.50026(3)	0.50159(2)	0.00298(1)
B1B2	-0.00250(2)	0.00051(2)	0.49693(2)	0.00251(1)
B2A1	0.74812(2)	0.75606(2)	0.25244(2)	0.00261(1)
B2A2	0.75903(2)	0.25194(2)	0.25345(2)	0.00241(2)
B2B1	0.00249(3)	0.74409(2)	0.75120(2)	0.00291(1)
B2B2	0.00217(3)	0.24621(2)	0.75129(2)	0.00246(1)
B31	0.87667(2)	0.87864(2)	0.37924(2)	0.00313(2)
B32	0.87634(2)	0.38689(2)	0.38042(2)	0.00281(2)
B33	0.62647(2)	0.88608(2)	0.12176(2)	0.00262(1)
B34	0.62854(2)	0.37465(2)	0.12317(2)	0.00257(2)
B41	0.87610(2)	0.62510(2)	0.37643(2)	0.00259(2)
B42	0.87560(2)	0.13092(2)	0.37423(2)	0.00280(2)
B43	0.62602(2)	0.62727(2)	0.12570(2)	0.00253(1)
B44	0.62788(2)	0.12528(3)	0.12614(2)	0.00280(1)
O11	0.8755(1)	0.8782(1)	-0.00018(8)	0.00432(1)
O12	0.8755(1)	0.3789(1)	-0.00170(8)	0.0038(1)
O13	0.6261(1)	0.8827(1)	0.50454(7)	0.00297(8)
O14	0.6250(1)	0.38391(9)	0.50523(7)	0.00272(8)
O21	0.8764(1)	0.6235(1)	0.00032(8)	0.0038(1)
O22	0.8769(1)	0.1242(1)	0.00047(8)	0.0038(1)
O23	0.6234(1)	0.6222(1)	0.50416(8)	0.0041(1)
O24	0.6257(1)	0.1240(1)	0.50264(8)	0.0037(1)
O31	0.8777(1)	0.86809(7)	0.25346(7)	0.00299(8)
O32	0.8740(1)	0.37387(9)	0.25575(7)	0.00371(9)
O33	0.6294(1)	0.87772(9)	0.24655(7)	0.00347(9)
O34	0.6250(1)	0.37171(9)	0.24642(8)	0.0044(1)
O41	0.8767(1)	0.63732(7)	0.25440(6)	0.00318(8)
O42	0.8777(1)	0.13236(8)	0.25168(8)	0.00365(9)
O43	0.6286(1)	0.63106(9)	0.24630(8)	0.0046(1)

O44	0.6265(1)	0.13583(9)	0.24877(8)	0.0045(1)
O5A1	0.7437(1)	0.75061(9)	0.13004(6)	0.00320(8)
O5A2	0.7484(1)	0.25600(9)	0.12997(7)	0.00348(9)
O5A3	0.7531(1)	0.7548(1)	0.37202(7)	0.0044(1)
O5A4	0.7560(1)	0.2570(1)	0.37401(8)	0.0047(1)
O5B1	0.0097(1)	0.7487(1)	0.62877(7)	0.00326(9)
O5B2	0.0051(1)	0.2458(1)	0.63022(7)	0.00365(9)
O5B3	-0.0053(1)	0.7460(1)	0.87181(7)	0.0039(1)
O5B4	-0.0027(1)	0.2438(1)	0.87105(6)	0.00371(9)
O6A1	0.74311(9)	0.5032(1)	0.12558(7)	0.00382(9)
O6A2	0.7509(1)	0.0007(1)	0.12427(7)	0.0044(1)
O6A3	0.7526(1)	0.5016(1)	0.37612(6)	0.00333(8)
O6A4	0.7594(1)	0.0033(1)	0.37649(7)	0.00349(9)
O6B1	0.0110(1)	-0.0023(1)	0.62355(7)	0.00434(9)
O6B2	0.0027(1)	0.4990(1)	0.62591(7)	0.00439(9)
O6B3	-0.0028(1)	-0.0022(1)	0.87641(7)	0.00351(8)
O6B4	0.0004(1)	0.4982(1)	0.87740(7)	0.00363(8)

Table S3 - Anisotropic thermal parameters.

Sites	**U11 (Å^2)**	**U22 (Å^2)**	**U33 (Å^2)**	**U23 (Å^2)**	**U13 (Å^2)**	**U12 (Å^2)**
A11	0.00280(3	0.00248(3	0.00157(3	-0.00009(3)	0.00010(2)	0.0000(3)
A12	0.00273(3	0.00224(3	0.00152(3	-0.00009(3)	0.00011(2)	0.00006(3)
A13	0.00298(4	0.00216(3	0.00209(3	-0.00027(3)	0.00039(3)	-0.00010(3)
A14	0.00300(3	0.00182(3	0.00213(3	-0.00024(3)	0.00041(2)	0.0000(3)
A21	0.00274(4	0.00209(3	0.00172(3	-0.00024(3)	0.00020(2)	-0.00008(3)
A22	0.00250(4	0.00184(3	0.00210(3	0.00004(2)	0.00027(2)	0.00003(2)
A23	0.00300(3	0.00240(3	0.00203(3	-0.00013(3)	0.00032(3)	-0.00001(3)
A24	0.00263(4	0.00255(3	0.00212(3	-0.00027(3)	0.00021(2)	0.00002(3)
B1A1	0.00339(3	0.00245(3	0.00259(2	-0.00046(2)	-0.00004(2)	0.00021(2)
B1A2	0.00314(3	0.00249(3	0.00236(2	-0.00038(2)	0.00007(2)	0.00037(2)
B1B1	0.00372(3	0.00255(2	0.00269(3	0.00048(1)	0.00111(2)	0.00027(1)
B1B2	0.00306(3	0.00234(2	0.00215(3	0.00019(3)	0.00045(2)	0.00002(2)
B2A1	0.00364(3	0.00214(3	0.00206(3	-0.00013(2)	0.00014(2)	-0.00023(3)
B2A2	0.00271(3	0.00251(3	0.00203(3	-0.00012(2)	0.00014(2)	0.00017(2)
B2B1	0.00417(2	0.00256(2	0.00201(2	-0.00013(3)	0.00049(2)	-0.00013(4)
B2B2	0.00282(2	0.00254(2	0.00202(2	-0.00015(3)	0.00035(1)	-0.00008(3)
B31	0.00348(3	0.00321(3	0.00271(4	0.00055(3)	0.00081(3)	0.00047(3)
B32	0.00313(2	0.00300(3	0.00229(3	0.00017(3)	0.00020(3)	-0.00008(3)
B33	0.00313(3	0.00256(3	0.00217(3	-0.00025(3)	0.00020(3)	-0.00006(3)

B34	0.00310(3	0.00237(3	0.00223(4	-0.00020(3)	0.00005(3)	0.00014(3)
B41	0.00291(3	0.00303(3	0.00184(4	0.0000(3)	0.0001(3)	0.00012(3)
B42	0.00362(3	0.00227(3	0.00253(4	-0.00050(3)	0.00084(3)	-0.00041(3)
B43	0.00311(3	0.00246(3	0.00202(3	-0.00018(2)	0.00034(2)	-0.00004(2)
B44	0.00297(3	0.00304(3	0.00239(3	-0.00047(2)	0.00043(2)	0.00026(3)
O11	0.0051(2)	0.0037(2)	0.0043(2)	0.0019(2)	0.0005(2)	-0.0005(2)
O12	0.0044(2)	0.0027(2)	0.0041(2)	0.0014(1)	0.0006(2)	-0.0004(2)
O13	0.0042(2)	0.0022(2)	0.0025(2)	-0.0001(1)	-0.0001(1)	0.0001(1)
O14	0.0044(2)	0.0017(1)	0.0021(2)	-0.0005(1)	0.0004(1)	0.0005(1)
O21	0.0045(2)	0.0039(2)	0.0031(2)	-0.0015(1)	0.0002(1)	0.0005(2)
O22	0.0051(2)	0.0032(2)	0.0032(2)	-0.0017(1)	0.0000(2)	0.0007(1)
O23	0.0057(2)	0.0033(2)	0.0033(2)	-0.0002(1)	0.0010(2)	-0.0002(2)
O24	0.0048(2)	0.0031(2)	0.0033(2)	-0.0003(1)	0.0005(2)	0.0004(2)
O31	0.0044(2)	0.0009(1)	0.0037(2)	-0.0007(2)	0.0002(1)	0.0002(1)
O32	0.0042(2)	0.0040(2)	0.0029(2)	0.0004(1)	-0.0004(1)	-0.0001(2)
O33	0.0046(2)	0.0021(1)	0.0037(2)	-0.0008(1)	0.0003(1)	0.0004(1)
O34	0.0047(2)	0.0046(2)	0.0040(2)	-0.0002(2)	0.0004(2)	0.0004(2)
O41	0.0050(2)	0.0020(1)	0.0028(2)	-0.0011(1)	0.0004(1)	0.0001(1)
O42	0.0048(2)	0.0022(2)	0.0039(2)	0.0001(1)	0.0000(1)	-0.0001(1)
O43	0.0053(2)	0.0046(2)	0.0040(2)	-0.0007(1)	0.0002(1)	0.0004(2)
O44	0.0038(2)	0.0057(2)	0.0040(2)	-0.0003(2)	0.0002(1)	0.0004(2)
O5A1	0.0043(2)	0.0029(1)	0.0024(1)	-0.0003(1)	0.0007(1)	0.0001(1)
O5A2	0.0044(2)	0.0032(2)	0.0029(2)	-0.0004(1)	0.0005(1)	0.0008(1)
O5A3	0.0034(2)	0.0059(2)	0.0040(2)	-0.0004(2)	0.0004(1)	0.0004(2)
O5A4	0.0043(2)	0.0050(2)	0.0048(2)	0.0001(1)	0.0008(1)	-0.0001(1)
O5B1	0.0036(2)	0.0036(2)	0.0025(2)	0.0001(1)	0.0002(1)	-0.0001(1)
O5B2	0.0034(2)	0.0044(2)	0.0032(2)	0.0007(1)	0.0000(1)	-0.0003(1)
O5B3	0.0039(2)	0.0039(2)	0.0038(2)	-0.0004(1)	-0.0004(1)	0.0002(1)
O5B4	0.0044(2)	0.0036(2)	0.0032(2)	-0.0010(1)	-0.0003(1)	-0.0004(1)
O6A1	0.0034(2)	0.0038(2)	0.0042(2)	0.0003(2)	-0.0006(1)	-0.0002(2)
O6A2	0.0041(2)	0.0053(2)	0.0038(2)	0.0001(2)	0.0001(1)	0.0001(2)
O6A3	0.0039(2)	0.0034(2)	0.0027(1)	-0.0003(1)	-0.0002(1)	-0.0001(1)
O6A4	0.0034(2)	0.0038(2)	0.0033(1)	0.0003(2)	0.0002(1)	-0.0003(2)
O6B1	0.0040(2)	0.0043(2)	0.0047(2)	-0.0004(2)	0.0008(1)	0.0001(1)
O6B2	0.0040(2)	0.0055(2)	0.0036(2)	-0.0001(2)	0.0008(1)	0.0000(2)
O6B3	0.0044(2)	0.0031(2)	0.0031(2)	-0.0001(1)	0.0005(1)	0.0002(1)
O6B4	0.0047(2)	0.0029(2)	0.0033(2)	0.0001(2)	0.0003(1)	0.0000(2)

Table S4 - Distortion mode and Bond Valence Sum values for the natural magnetite crystal, for each iron B-site. The comparison with the original model is set so that (Δ = (pure value) − (natural value)). Starred/unstarred BVS values show Fe^{3+}/Fe^{2+}-like states

Site	Q_{rad} (Å)	ΔQ_{rad} (Å)	Q_{JT} (Å)	ΔQ_{JT} (Å)	Q_O (Å)	ΔQ_O (Å)	BVS	ΔBVS
B1B1	0.036	0.002	-0.036	-0.002	-0.001	-0.003	2.48	-0.01
B31	-0.002	0.009	-0.018	0.010	-0.019	-0.001	2.61*	-0.03
B32	-0.006	0.009	0.001	0.015	0.003	-0.002	2.64*	-0.03
B1A1	0.039	-0.003	-0.018	-0.010	-0.025	-0.001	2.47	0.01
B1A2	0.047	-0.001	-0.049	0.001	-0.003	-0.005	2.44	0.00
B33	0.002	-0.005	-0.012	0.021	-0.007	0.017	2.63*	0.01
B41	0.054	-0.005	-0.050	0.021	-0.006	-0.023	2.43	0.01
B2A1	-0.045	-0.002	-0.009	-0.001	-0.008	0.000	2.77*	0.00
B34	-0.054	-0.005	0.013	-0.005	0.004	0.000	2.80*	0.01
B1B2	0.013	0.002	-0.018	-0.008	-0.011	0.003	2.57	-0.01
B43	-0.092	0.002	0.003	-0.007	0.002	-0.005	2.94*	-0.01
B2B2	-0.089	-0.008	0.005	0.003	0.002	-0.001	2.93*	0.03
B44	0.058	0.007	-0.043	-0.014	-0.011	0.008	2.41	-0.03
B42	0.022	-0.003	-0.046	-0.012	-0.004	0.002	2.53	0.01
B2B1	0.032	0.005	-0.047	0.008	-0.006	-0.012	2.50	-0.02
B2A2	-0.016	0.000	0.009	0.007	0.017	-0.011	2.69*	-0.01